Progress In Electromagnetics Research C, Vol. 64, 89–96, 2016

A UHF Third Order 5-bit Digital Tunable Bandpass Filter Based on Mixed Coupled Open Ring Resonators

Ming-Ye Fu, Qian-Yin Xiang*, Dan Zhang, Deng-Yao Tian, and Quan-Yuan Feng

Abstract—This paper presents a third-order digital tunable bandpass filter based on digitally tunable capacitor loaded microstrip open ring resonator. Magnetic dominated mixed coupling is utilized to make the coupling coefficient meet the requirement of stable bandwidth response. Electric source-load coupling is designed to generate a transmission zero for improving the frequency selectivity. This filter is designed, fabricated and measured. The measurement shows that the filter can be digitally tuned by 5-bits pure digital command. The fractional bandwidth is $9 \pm 1\%$, and the tuning range is from 410 MHz to 820 MHz.

1. INTRODUCTION

With the fast development of wireless technology, miniaturization of radio frequency components is highly demanded. Thus the design of tunable components such as a tunable filter becomes a popular research topic for multi-band or frequency agile wireless systems [1–4]. Most of today's tunable filters are designed based on either mechanical, magnetic, or electrically tunable resonators. Mechanical and magnetic ones have high quality factor; however, their bulkiness, cost, tuning speed limit their modern applications [5]. For electrical tunable filters, the tunable/switchable components are mainly semiconductor varactors diodes, PIN diodes, and RF MEMS, among which, semiconductor varactor diodes are the most popular ones because of their fast tuning speed and low cost [6–16]. However, they suffer from poor linearity [9]. Besides, semiconductor varactor diodes need high analogue voltage sources to bias the PN junction, and there is a limited power handling capability, as well. PIN diodes with high switch on power consumption also need high voltage bias source [17]. RF MEMS has been used to design tunable RF devices [2, 18–21]. However, RF MEMS have complicated biasing schemes, stringent processing and packaging requirements. Recently, semiconductor digitally tunable capacitors (DTCs) are available on the market [22]. These DTCs can be used to design digitally tunable RF filters and antenna impedance matching networks [23, 24]. Due to their high power handling capability, small size and fast tuning speed, DTCs will be essential components for future tunable RF filters.

Open-ring resonator (ORR) is one of the modified forms of half wave-length uniform resonator and is widely used with good performance [25, 26]. In this paper, DTC loaded ORRs are used to design a third order microstrip tunable filter. Based on the third order magnetic dominated mixed coupling, magnetic feeding, and electric source-load coupling, a high side transmission zero is generated to improve the frequency selectivity. The filter can be controlled by the microprocessor based digital control board directly. The filter is designed, fabricated and measured. In Section 2, the basic design theory is presented. Sections 3 and 4 discuss the simulation and measurement, respectively. A conclusion is given in Section 5.

Received 27 March 2016, Accepted 11 May 2016, Scheduled 22 May 2016
* Corresponding author: Qian-Yin Xiang (qyxiang@swjtu.edu.cn).
The authors are with the School of Information Science and Technology, Southwest Jiaotong University, Chengdu 611756, China.

2. FILTER DESIGN

The configuration of the proposed tunable bandpass filter with DTC loaded ORRs is shown in Figure 1(a). DTC is loaded at the split of the ORR. Magnetic dominated mixed coupling is utilized to meet the requirement of constant fractional bandwidth, and magnetic feeding is implemented to achieve impedance matching across a wide tuning range. Meanwhile, multiple coupling path, which can cause several signals cancel each other at a certain frequency, can be used to generate transmission zeros [27]. In this design, electric source-load coupling is introduced to generate a high-side transmission zero for improving the frequency selectivity. The coupling topology of the filter is shown in Figure 1(b). A phase shift of $-\pi/2$ can be obtained through the source-load coupling path at the high frequency side of the resonating frequency, and the phase shift from source to load through the coupling of resonators is $\pi/2\,(=\pi/2-\pi/2+\pi/2-\pi/2+\pi/2-\pi/2+\pi/2)$. Therefore, the two waves cancel each other. As a result, a high side zero can be generated.

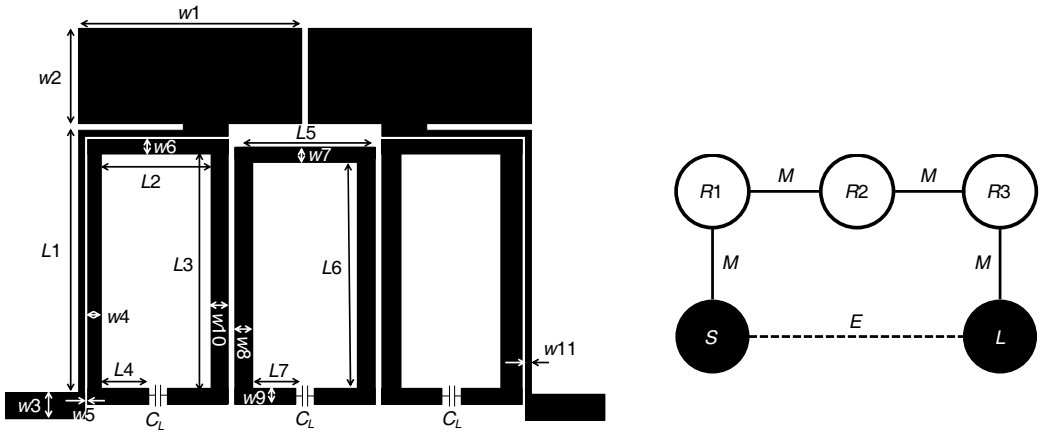

Figure 1. The proposed third order tunable filter: (a) the configuration, (b) the coupling topology.

The required coupling coefficient $k_{i,j}$ can be given by:

$$M_{i,j} = \frac{k_{i,j}}{\text{FBW}} \tag{1}$$

where FBW is the filter's fractional bandwidth, and $k_{i,j}$ is the coupling coefficient between the ith and jth resonators. $M_{i,j}$ is a constant for a specific response. In order to achieve constant fractional bandwidth (CFBW), from Equation (1) it shows that the coupling coefficient should be unchanged while the center frequency varies.

To obtain the desired coupling coefficient, mixed coupled tunable half-wavelength OORs are utilized in the proposed filter. The electric and magnetic coupling between the resonators can be evaluated by studying the voltage and current distributions [28]. Ignoring the parasitic effects, the DTC can be equivalent to a segment of open-ended microstrip line [29]. Figure 2(a) shows the normalized voltage and current distributions of the resonator under different DTC capacitance. The middle part with the length of L denotes the passive microstrip line of the resonator. ΔL_1 and ΔL_2 are used to represent the DTC with different capacitance. The length of the coupled region is d. When the capacitance of the DTC is larger, the equivalent microstrip line is longer and the resonant frequency is lower. At the fundamental resonant frequency, the normalized voltage and current distribution under minimized and maximum DTC capacitances are given in Figure 2(a). The electric and magnetic coupling coefficient can be given as [29]:

$$k_e = p\int_d^{d+\Delta d} |V|^2 dl \tag{2}$$

$$k_m = p\int_d^{d+\Delta d} |I|^2 dl \tag{3}$$

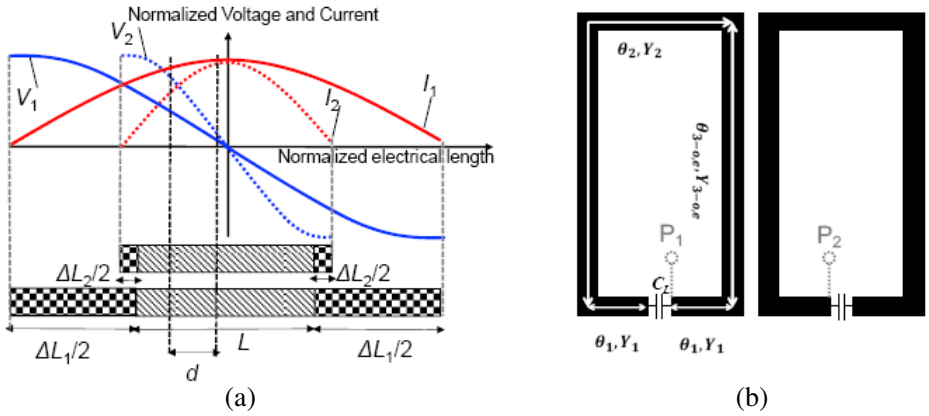

Figure 2. (a) Normalized voltage and current distributions on the tunable resonator under low and high frequency, (b) the analysis model of the coupled resonators.

The total coupling coefficient can be obtained as:

$$k = |k_m - k_e| \tag{4}$$

In the coupling region, it can be seen from Figure 2(a) that the magnetic coupling increases, and the electric coupling decreases when the tunable capacitance increases. Therefore, the overall coupling coefficient is slightly increased when the resonant frequency is decreased.

Y matrix is used to calculate the resonant frequency and coupling factor. In order to calculate the Y matrix of this proposed filter, the microstrip line of each resonator can be divided into four segments, as shown in Figure 2(b). For each microstrip line, the $ABCD$ matrix is given as follows:

$$A_{\text{line\_}c} = \begin{pmatrix} \cos\theta_c & j\frac{1}{Y_c}\sin\theta_c \\ jY_c\sin\theta_c & \cos\theta_c \end{pmatrix} \tag{5}$$

where Y_c is the characteristic admittance of each type of the microstrip line with an electric length of θ_c, here $c = 1$, 2, and 3. By using even and odd method, the $ABCD$ matrix of the microstrip line of the resonator shown in Figure 2(b) can be written as:

$$A_{\text{line}(e,o)} = A_{\text{line\_1}} \cdot A_{\text{line\_3}(e,o)} \cdot A_{\text{line\_2}} \cdot A_{\text{line\_1}} \tag{6}$$

where, the subscript (e, o) stands for the even or odd mode.

Therefore, without considering the loaded capacitor C_L, the Y matrixes of the microstrip line of each resonator can be expressed as:

$$Y_{\text{line}(e,o)} = \begin{pmatrix} A_{\text{line22}(e,o)}/A_{\text{line12}(e,o)} & -\Delta A_{\text{line}(e,o)}/A_{\text{line12}(e,o)} \\ -1/A_{\text{line12}(e,o)} & -A_{\text{line11}(e,o)}/A_{\text{line12}(e,o)} \end{pmatrix} \tag{7}$$

where, Δ is the determinant operator. Meanwhile, the admittance matrix of the loaded capacitor C_L is:

$$Y_{C_L} = \begin{pmatrix} j\omega C_L & -j\omega C_L \\ -j\omega C_L & j\omega C_L \end{pmatrix} \tag{8}$$

Since the loaded capacitor C_L is connected to the microstrip lines in parallel, the total admittance matrix of each resonator $Yt = Y_{\text{line}} + Y_{C_L}$, the even and odd mode of Yt can be written as:

$$Yt_{(e,o)} = \begin{pmatrix} A_{\text{line22}(e,o)}/A_{\text{line12}(e,o)} + j\omega C_L & -\Delta A_{\text{line}(e,o)}/A_{\text{line12}(e,o)} - j\omega C_L \\ -1/A_{\text{line12}(e,o)} - j\omega C_L & -A_{\text{line11}(e,o)}/A_{\text{line12}(e,o)} + j\omega C_L \end{pmatrix} \tag{9}$$

The input admittance seen from port P_1 or P_2 is given as [30]:

$$Yin_{(e,o)} = \frac{Yt_{(e,o)}(1,1) \cdot Yt_{(e,o)}(2,2) - Yt_{(e,o)}(1,2) \cdot Yt_{(e,o)}(2,1)}{Yt_{(e,o)}(2,2)} \tag{10}$$

Therefore, the admittance matrix for each coupled resonator can be written as:

$$Y = \begin{pmatrix} \frac{Yin_e+Yin_o}{2} & \frac{Yin_e-Yin_o}{2} \\ \frac{Yin_e-Yin_o}{2} & \frac{Yin_e+Yin_o}{2} \end{pmatrix} \tag{11}$$

The resonant frequency ω_0 and coupling coefficient k can be calculated by the admittance matrix as [9]:

$$\mathrm{Im}\left[Y_{11}\left(\omega_0\right)\right] = 0 \tag{12}$$

$$k = \frac{\mathrm{Im}[Y_{12}(\omega_0)]}{b(\omega_0)} \tag{13}$$

where:

$$b(\omega) = \frac{\omega}{2}\frac{\partial \mathrm{Im}[Y_{11}(\omega)]}{\partial \omega} \tag{14}$$

Numerical calculation and simulation are used to verify the tunable capability. The simulation was carried out by using SONNET and ADS (*Advanced Design System*). Ideal capacitor C_L is used as the tunable capacitor, and the geometry parameters of the proposed filter shown in Figure 1(a) are: $W1 = 20.3$, $W2 = 10.5$, $W3 = 2.5$, $W4 = 1$, $W5 = 0.2$, $W6 = 1$, $W7 = 0.9$, $W8 = 0.9$, $W9 = 1.5$, $W10 = 0.9$, $W11 = 0.5$, $L1 = 30.6$, $L2 = 11.5$, $L3 = 29$, $L4 = 4.7$, $L5 = 11.5$, $L6 = 28.7$, and $L7 = 3.8$ (Unit: mm). F4B-2 ($h = 0.8$ mm, $\varepsilon_r = 2.65$, $\tan\theta = 0.001$) is selected as the substrate. Figure 3(a) shows that the center frequency of the filter can be changed by tuning the capacitor C_L, and Figure 3(b) shows that the coupling coefficient k is stable when the center frequency is tuned. Both the calculation and simulation shows that a stable fractional bandwidth response can be achieved by using the proposed tunable filter.

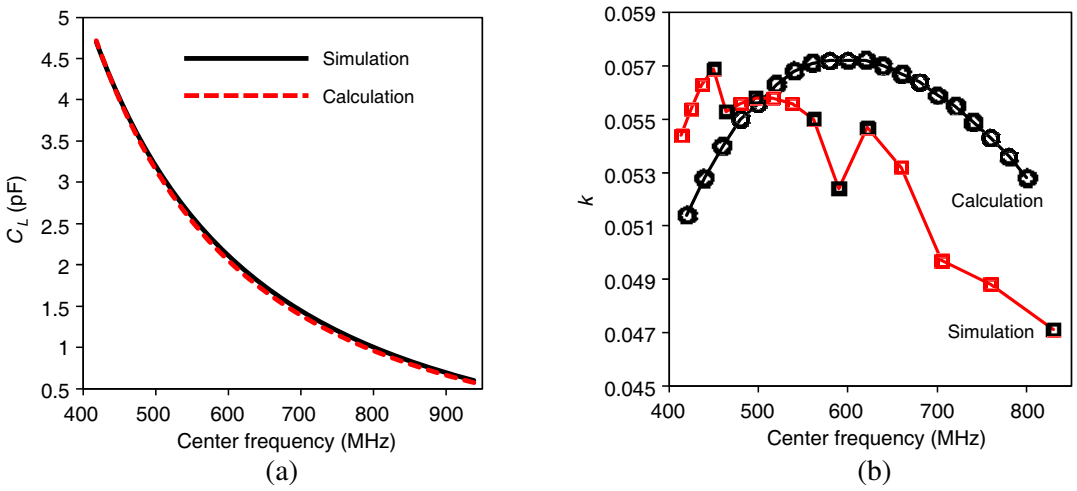

Figure 3. Simulated results based on ideal tunable capacitor: (a) center frequency tunable capability, (b) coupling coefficient k versus center frequency.

3. SIMULATION

The geometry parameters presented in the last section are used in the simulation. The 5-bit digitally tunable capacitor PE64904, with the tunable capacitance of 0.6 pF to 4.7 pF, is chosen as the tunable capacitor. Equivalent circuit model of PE64904 [22] is used in the circuit simulation. Figure 4(a) shows the package of PE64904, and Figure 4(b) shows the layout of it. Figure 5(a) shows the simulated scatter parameters of the filter. It shows that the passband of the filter can be tuned, and a transmission zero is located at the high side of the passband. Figure 5(b) summarizes the bandwidth versus center frequency for all the 32 states. It shows that the tuning range is from 410 MHz to 820 MHz. The fractional bandwidth increases from 7.5% to 10%, while the center frequency decreases.

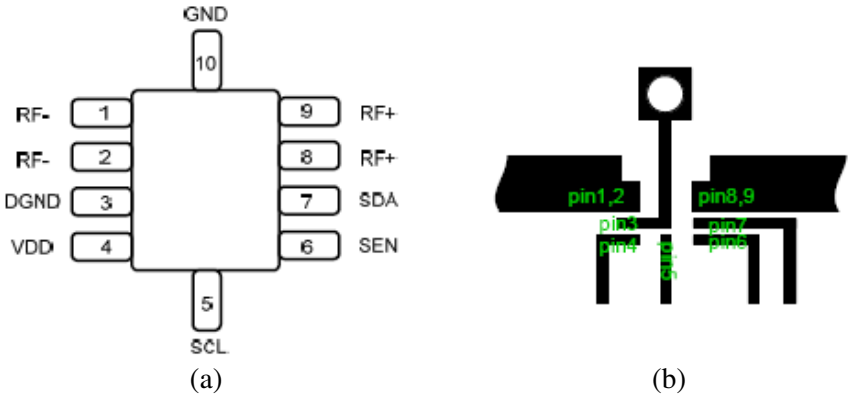

(a) (b)

Figure 4. (a) The package of PE64904, (b) layout of PE64904.

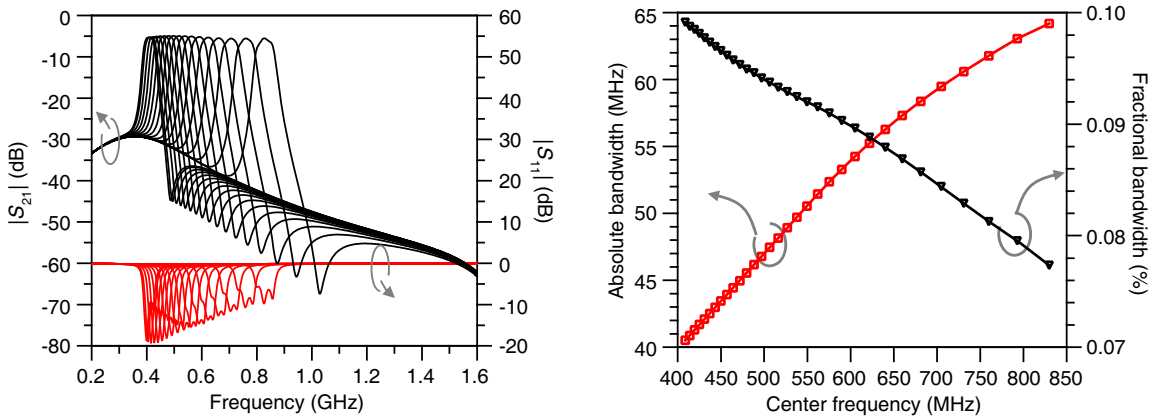

(a) (b)

Figure 5. Simulation results: (a) the tunable scatter responses, (b) the bandwidth versus center frequency.

4. FABRICATION AND MEASUREMENT

The filter is fabricated on an F4B-2 substrate ($h = 0.8\,\text{mm}$, $\varepsilon_r = 2.65$, $\tan\theta = 0.001$) with an overall size of $60\,\text{mm} \times 68.5\,\text{mm}$, as shown in Figure 6(a). The 5-bit DTC PE64904 is controlled by a MCU (STM8S103F3P6) based control board through SPI (Serial Peripheral Interface), as shown

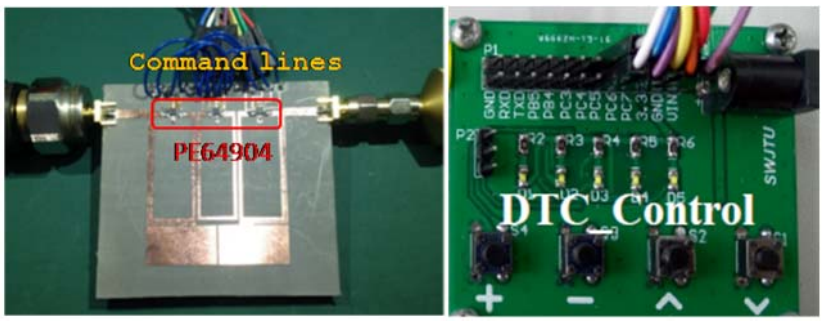

(a) (b)

Figure 6. (a) The fabricated digital tunable bandpass filter, (b) the control board.

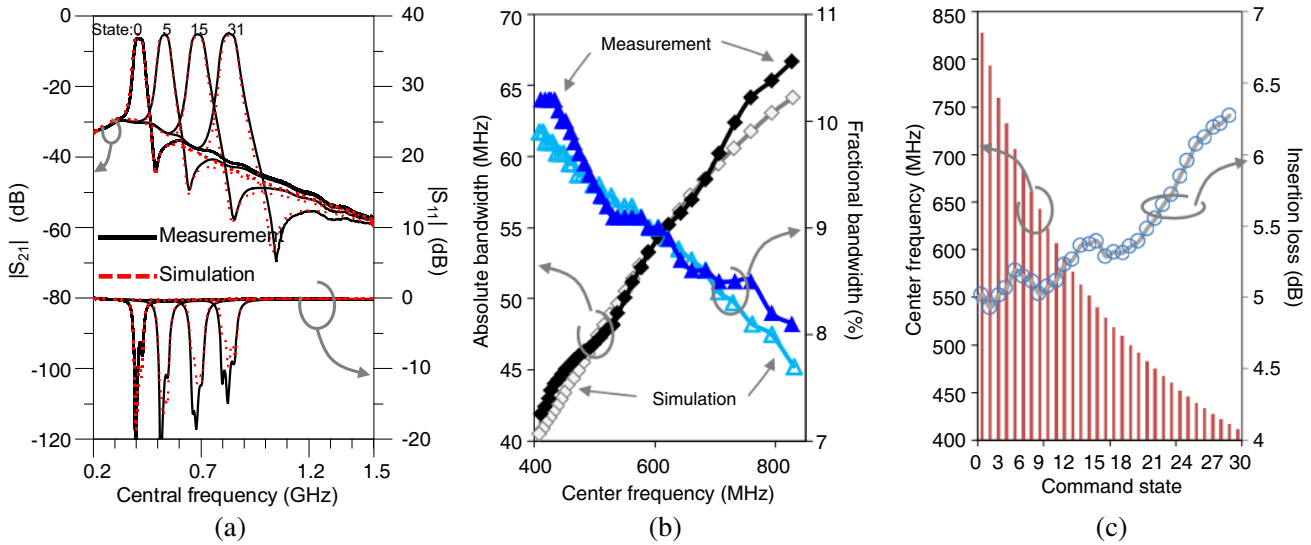

Figure 7. (a) The measured scatter parameters, (b) the measured bandwidth versus the center frequency, (c) the center frequency and insertion loss versus the command state.

Table 1. Comparison with related works.

Reference	Order	Tuning device	Tunable range	Bandwidth	Insertion loss	Foot print
[23]	$N = 2$	DTC	0.52–0.86 GHz	110 ± 5 MHz*	4.8–3 dB	24 mm × 19 mm
[26]	$N = 3$	Varactor diode	1.1–1.88 GHz	90 ± 8 MHz*	6.8–4.3 dB	40 mm × 36 mm
[31]	$N = 3$	Varactor diode	1.75–2.25 GHz	95 ± 10 MHz$^+$	7.2–3.2 dB	10.4 mm × 14.8 mm
This work	$N = 3$	DTC	0.41–0.82 GHz	54 ± 12 MHz $(9 \pm 1\%)$*	6.5–4.9 dB	60 mm × 68.5 mm

*-3 dB bandwidth, $^+$-1 dB bandwidth

in Figure 6(b). There is no analog control circuit required, and the filter can be tuned digitally. The frequency response of the filter is measured by Agilent E5071C vector network analyzer.

Figure 7(a) shows the measured and simulated S-parameters of the filter at state 0, 5, 15, and 31. A transmission zero is located at the upper stop band. The rejection level is larger than 40 dB. Figure 7(b) shows the measured and simulated bandwidth versus the center frequency. Figure 7(c) shows the center frequency and insertion loss under all the 32 digital command states. The simulation matches the measurement very well. The result shows that the fractional bandwidth is about $9 \pm 1\%$, and the insertion loss is less than 6.5 dB for all the states. The absolute bandwidth is 54 ± 12 MHz over the center frequency tuning range from 410 MHz to 820 MHz, and an octave tunable capability is achieved. The comparison with related works is summarized in Table 1.

5. CONCLUSION

Digitally tunable capacitor loaded open ring resonator with mixed coupling is utilized to design a third order 5-bit digital tunable filter. Based on the magnetic dominated mixed coupling, electric source-load coupling is designed to generate a high side transmission zero for improving the frequency selectivity of the proposed filter. The measured results show that the filter can be digitally tuned with 5-bits, the fractional bandwidth is $9 \pm 1\%$, and an octave tuning range from 410 MHz to 820 MHz is achieved. Simulations and measurements are in excellent agreement for this filter. The proposed filter can be used in the digital reconfigurable RF front-end of wideband frequency agile systems.

ACKNOWLEDGMENT

This work was supported by the National Natural Science Foundation of China (NSFC) under Grant 61401375, 61504110, 61271090, the Fundamental Research Funds for the Central Universities under Grant 2682014RC24, 2682015CX065, and the Sichuan Province Science and Technology Support Program 2015GZ0103, 2016GZ0059.

REFERENCES

1. Asadi, H., H. Volos, M. M. Marefat, and T. Bose, "Metacognition and the next generation of cognitive radio engines," *IEEE Communications Magazine*, Vol. 54, No. 1, 76–82, 2016
2. Abbaspour-Sani, E., N. Nasirzadeh, and G. R. Dadashzadeh, "Two novel structures for tunable MEMS capacitor with RF applications," *Progress In Electromagnetics Research*, Vol. 68, 169–183, 2007.
3. Gao, L., X. Y. Zhang, and Q. Xue, "Compact tunable filtering power divider with constant absolute bandwidth," *IEEE Trans. Microw. Theory Tech.*, Vol. 63, No. 10, Oct. 2015
4. Xiang, Q., Q. Feng, X. Huang, and D. Jia, "Electrical tunable microstrip LC bandpass filters with constant bandwidth," *IEEE Trans. Microw. Theory Tech.*, Vol. 61, No. 3, 1124–1130, 2013.
5. Uher, J. and W. J. R. Hoefer, "Tunable microwave and millimeter-wave bandpass filters," *IEEE Trans. Microw. Theory Tech.*, Vol. 39, 643–653, Apr. 1991.
6. Xiang, Q., Q. Feng, and X. Huang, "Half-mode substrate integrated waveguide (HMSIW) filters and its application to tunable filters," *Journal of Electromagnetic Waves and Applications*, Vol. 25, 2043–2053, 2011.
7. Huang, X., L. Zhu, Q. Feng, Q. Xiang, and D. Jia, "Tunable bandpass filter with independently controllable dual passbands," *IEEE Trans. Microw. Theory Tech.*, Vol. 61, No. 9, 3200–3208, Sep. 2013.
8. Xiang, Q., Q. Feng, and X. Huang, "Substrate integrated waveguide filters and mechanical/electrical reconfigurable half-mode substrate integrated waveguide filters," *Journal of Electromagnetic Waves and Applications*, Vol. 26, 1756–1766, 2012.
9. El-Tanani, M. A. and G. M. Rebeiz, "A two-pole two-zero tunable filter with improved linearity," *IEEE Trans. Microw. Theory Tech.*, Vol. 57, No. 4, Apr. 2009.
10. Zhang, X. Y., C. H. Chan, Q. Xue, and B.-J. Hu, "RF tunable bandstop filters with constant bandwidth based on a doublet configuration," *IEEE Trans. Ind. Electron.*, Vol. 59, No. 2, 1257–1265, Feb. 2012.
11. Luo, X., S. Sun, and R. B. Staszewski, "Tunable bandpass filter with two adjustable transmission poles and compensable coupling," *IEEE Trans. Microw. Theory Tech.*, Vol. 62, No. 9, 2003–2013, Set. 2014.
12. Wang, Y., F. Wei, H. Xu, and X.-W. Shi, "A tunable 1.4–2.5 GHz bandpass filter based on single mode," *Progress In Electromagnetics Research*, Vol. 135, 261–269, 2013.
13. Chen, J.-X., J. Shi, Z.-H. Bao, and Q. Xue, "Tunable and switchable bandpass filters using slot-line resonators," *Progress In Electromagnetics Research*, Vol. 111, 25–41, 2011.
14. Xiang, Q.-Y., Q. Feng, X.-G. Huang, and D.-H. Jia, "A novel microstrip L_c reconfigurable bandpass filter," *Progress In Electromagnetics Research Letters*, Vol. 36, 171–179, 2013.
15. Cao, L., G. Li, J. Hu, and L. Yin, "A miniaturized tunable bandpass filter with constant fractional bandwidth," *Progress In Electromagnetics Research C*, Vol. 57, 89–97, 2015.
16. Jia, D.-H., Q. Feng, X.-G. Huang, and Q.-Y. Xiang, "A dual-band bandpass filter with a tunable passband," *Progress In Electromagnetics Research C*, Vol. 37, 107–118, 2013.
17. Tu, W.-H., "Compact low-loss reconfigurable bandpass filter with switchable bandwidth," *IEEE Microw. Wireless Compon. Lett.*, Vol. 20, No. 4, 208–210, Apr. 2010.
18. Ur Rehman, M. Z., Z. Baharudin, M. A. Zakariya, M. H. M. Khir, M. T. Jilani, and M. T. Khan, "RF MEMS based half mode bowtie shaped substrate integrated waveguide tunable bandpass filter," *Progress In Electromagnetics Research C*, Vol. 60, 21–30, 2015.

19. Young, R. M., J. D. Adam, et al., "Low-loss bandpass RF filter using MEMS capacitance switches to achieve a one-octave tuning range and independently variable bandwidth," *IEEE MTT-S Int. Microw. Symp. Dig.*, Vol. 3, 1781–1784, 2003.
20. Park, S. J., K. Y. Le, and G. M. Rebeiz, "Low-loss 5.15–5.70-GHz RF MEMS switchable filter for wireless LAN applications," *IEEE Trans. Microw. Theory Tech.*, Vol. 54, No. 11, 3931–3939, Nov. 2006.
21. El-Tanani, M. A. and G. M. Rebeiz, "High-performance 1.5–2.5-GHz RF-MEMS tunable filters for wireless applications," *IEEE Trans. Microw. Theory Tech.*, Vol. 58, No. 6, Jun. 2010
22. PE64904: 5-bit 32-state Digitally Tunable Capacitor, 100–3000 MHz, Peregrine Semiconductor, 9380 Carroll Park Drive, San Diego, CA 921921, USA.
23. Jaschke, A., M. Tessema, M. Schuhler, and R. Wansch, "Digitally tunable bandpass filter for cognitive radio applications," *IEEE 17th International Workshop on Computer Aided Modeling and Design of Communication Links and Networks*, 338–342, 2012.
24. Ranta, T. and R. Novak, "New tunable technology for mobile-TV antennas," *Microwave Journal*, Nov. 2008.
25. Gao, L., X. Y. Zhang, B.-J. Hu, and Q. Xue, "Novel multi-stub loaded resonators and their applications to various bandpass filters," *IEEE Trans. Microw. Theory Tech.*, Vol. 62, No. 5, May 2014.
26. Zhao, Z., J. Chen, L. Yang, and K. Chen, "Three-pole tunable filters with constant bandwidth using mixed combline and split-ring resonators," *IEEE Microw. Wireless Compon. Lett.*, Vol. 24, No. 10, Oct. 2014.
27. Chiou, Y.-C. and G. M. Rebeiz, "Tunable 1.55–2.1 GHz 4-pole elliptic bandpass filter with bandwidth control and $>$ 50 dB rejection for wireless systems," *IEEE Trans. Microw. Theory Tech.*, Vol. 61, No. 1, 117–124, Jan. 2013.
28. Dai, G. L., X. Y. Zhang, C. H. Chan, Q. Xue, and M. Y. Xia, "An investigation of open- and short-ended resonators and their applications to bandpass filters," *IEEE Trans. Microw. Theory Tech.*, Vol. 57, No. 9, 2203–2210, Sep. 2009.
29. Zhang, X. Y., Q. Xue, C. H. Chan, and B.-J. Hu, "Low-loss frequency-agile bandpass filters with controllable bandwidth and suppressed second harmonic," *IEEE Trans. Microw. Theory Tech.*, Vol. 58, No. 6, 1557–1564, Jun. 2010
30. Huang, X., Q. Feng, L. Zhu, and Q. Xiang, "A constant absolute bandwidth tunable filter using varactor-loaded open-loop resonators," *Asia-Pacific Microwave Conference Proceedings 2013*, 872–874, 2013
31. Chiou, Y. C. and G. M. Rebeiz, "A quasi elliptic function 1.75–2.25 GHz 3-pole bandpass filter with bandwidth control," *IEEE Trans. Microw. Theory Tech.*, Vol. 60, No. 2, 244–249, Feb. 2012.